Dalton Transactions

PAPER

View Article Online
View Journal

Cite this: DOI: 10.1039/c6dt00941g

Lead ion induced chemodosimeter approach of a tripodal hydroxyl-quinoline based phospho-ester through P–O bond cleavage†

Dibyendu Sain,‡ Chanda Kumari, Ashish Kumar, Hari Pada Nayek and Swapan Dey*

Received 9th March 2016,
Accepted 25th April 2016

DOI: 10.1039/c6dt00941g

www.rsc.org/dalton

Lead ion induced P–O bond breaking with instant colour change was observed in a tripodal hydroxyl-quinoline based phosphor-ester (**HQP**). A new penta-coordinated lead chelate complex $[Pb_4HQ_6(ClO_4)_2]$ was found. The hydrolysis reaction followed by P–O bond cleavage with 'Pb–O' and 'Pb–N' bond formation proved the chemodosimeter approach.

Introduction

Phospho-ester containing compounds have significant roles in a variety of biological processes as major constituents of nucleic acids and nucleotides.[1] These compounds have electron accepting tendencies to the 'P' centre, which promotes nucleophiles to attack,[2] leading to phospho-ester (P–O) bond cleavage.[3] There are lots of previous reports on P–O bond cleavage reactions.[4] A variety of research studies have also been focused on phosphate esters regarding their hydrolysis and alcoholysis reactions.[5] Selective nucleophilic attacks in phosphate esters and P–O bond cleavage reactions under acidic[6] and alkaline[7] conditions have been reported. 8-quinolyl phosphate and phosphate monoester are well known and the hydrolysis of the phosphate-ester by trivalent lanthanide ions has been employed to regulate biological activity.[8] The interaction between metal ions and nucleoside phosphates in chemistry and biochemistry is a well established phenomenon and the metal ion promoted reactions of phosphate derivatives have been thoroughly reviewed.[9] But still, there is no report of lead ion induced P–O bond cleavage reaction in a tripodal hydroxyl-quinoline based phospho-ester.

In this regard, chemodosimeters are employed to identify analyte selectively through irreversible chemical reaction with a signal which is observable to the naked eye.[10] The development of chemodosimeters for monitoring toxic metal cations has recently become an active research field.[11] In particular, lead(II) present in drinking water, has severe negative effects on physical and mental development of children.[12] It interferes with a variety of body processes and is toxic to many organs like the heart, bones, intestines, kidneys and reproductive system.[13] Therefore, the selective and rapid detection of Pb^{2+} in water or physiological samples is highly demanding and a challenging research area. A number of chemodosimeters have been previously reported for different metal ions[14] but still very few chemodosimeters are reported for the Pb^{2+} ion,[15] although, various chemosensors of Pb^{2+} ions based on peptide, protein and calixarene molecules have been reported previously.[16] For example, Ghosh *et al.* have recently described a triazole motif linked rhodamine-based chemosensor, which recognized both Hg^{2+} and Pb^{2+} ions.[17] Amino acid-based fluorescent chemosensors have also been designed and synthesized for the fluorescence turn-on detection of Pb^{2+} ions in aqueous media.[18]

Herein, we describe, for the first time, a Pb^{2+} induced P–O bond cleavage reaction of a 8-hydroxyquinoline based phospho-ester followed by the formation of a metal–chelate complex, $Pb_4(HQ)_6(ClO_4)_2$. Hydroxyquinoline phosphate (**HQP**) and naphthol phosphate (**NP**) were synthesized by the reaction of 8-hydroxyquinoline and 1-naphthol, accordingly, with $POCl_3$ in the presence of dry Et_3N (Scheme 1).

Results and discussion

X-ray crystallography analysis

Solid state structures of the **HQP**, **NP** and $Pb_4(HQ)_6(ClO_4)_2$ compounds were determined by X-ray crystallographic analysis. **HQP** crystallized in a cubic system with the *P*213 space group, whereas, **NP** was a monoclinic crystal system with the *P*21/*c* space group. The unit cells of both crystals contained

Department of Applied Chemistry, Indian School of Mines, Dhanbad, Jharkhand 826004, India. E-mail: dey.s.ac@ismdhanbad.ac.in, hpnayek@yahoo.com; Fax: +91 326 2296563; Tel: +91 326 2235607

†Electronic supplementary information (ESI) available: Experimental procedures, spectra, extensive tables, graphs and calculations. CCDC 1413010, 1413011 and 1413012 for **HQP**, $Pb_4HQ_6(ClO_4)_2$ and **NP**. For ESI and crystallographic data in CIF or other electronic format see DOI: 10.1039/c6dt00941g

‡Present address: College of Pharmacy, Sunchon National University, Suncheon, South Korea.

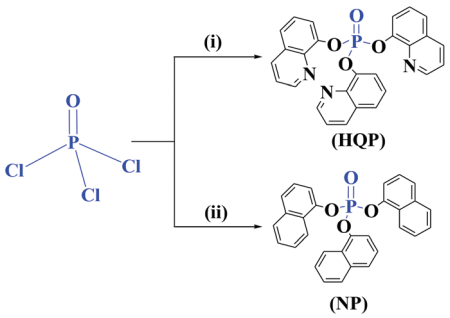

Scheme 1 Synthesis of **HQP** and **NP**. Reagents and conditions: dry Et_3N, dry benzene, reflux, 10 h, (i) 8-hydroxyquinoline, 70% yield; (ii) 1-naphthol, 75% yield.

four molecules ($Z = 4$). It was found that three quinoline and naphthalene moieties of **HQP** and **NP** respectively, were equidistance and far apart from each other. The P═O moiety was located at the apex of the molecule and the central P atom was connected with the three O atoms of the quinoline and naphthalene moieties of **HQP** and **NP** respectively (Fig. 1a and b). A new $\mathbf{Pb_4(HQ)_6(ClO_4)_2}$ chelate complex crystal was found, when $\mathbf{Pb(ClO_4)_2}$ was introduced with **HQP** in a CH_3OH–H_2O solvent with pH 2 to 3. It was a triclinic crystal with the $P\bar{1}$ space group. The structure showed that three P–O bonds of **HQP** were broken and four lead(II) ions were co-ordinated by six hydroxyquinoline (HQ) moieties through the Pb–O and Pb–N bonds (Fig. 1c). The three-dimensional network structure also displayed that all four lead atoms were penta co-ordinated and two of them were connected with two bridging moieties and one chelating HQ moiety (PbO_3N_2 unit), whereas the other two Pb atoms were attached to one bridging moiety and three chelating HQ moieties (PbO_4N unit). Two perchlorate counter anions (ClO_4^-) were connected with the $\mathbf{Pb_4(HQ)_6}$ unit through several short contacts (see ESI, Table S2†).

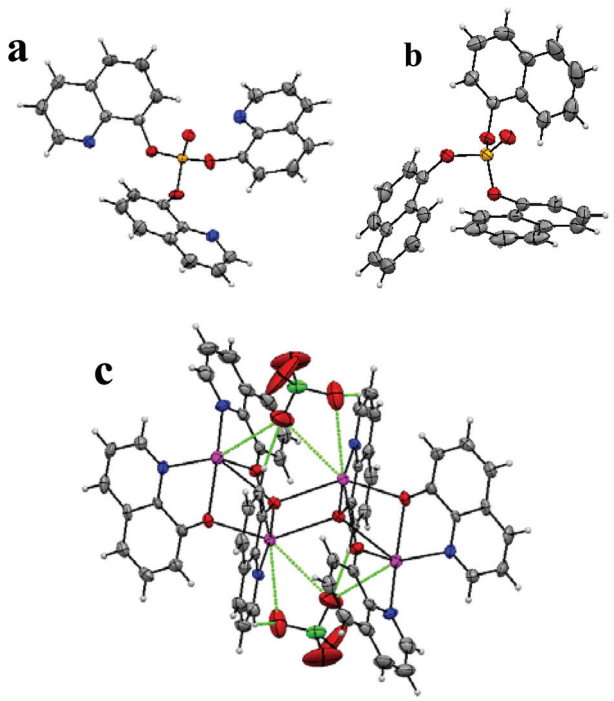

Fig. 1 Single crystal X-ray ORTEP diagrams of the (a) **HQP**, (b) **NP** and (c) $\mathbf{Pb_4(HQ)_6(ClO_4)_2}$ compounds (black for **C**, grey for **H**, blue for **N**, red for **O**, orange for **P**, green for **Cl** and pink for **Pb**).

Visual colour change experiment

The complexation study of **HQP** and **NP** was carried out with a series of perchlorate salts of Cu^{2+}, Zn^{2+}, Cd^{2+}, Hg^{2+}, Pb^{2+}, Bi^{3+} and Ag^{+} in CH_3OH–H_2O (1 : 1). **HQP** immediately changed its colour from colourless to yellowish green upon addition of 2.0 equivalents of $\mathbf{Pb^{2+}}$ (Fig. 2). **HQP** did not show any interesting response upon addition of a large excess of other cations, even up to 10.0 equivalents.

Complexation study using UV-vis experiments

The complexation studies using UV-Vis spectroscopy were recorded for **HQP** (2.08×10^{-4} M) with all mentioned cations in CH_3OH–H_2O (1 : 1). **HQP** itself showed absorption maxima at $\lambda_{max} = 281$ nm. With the gradual addition of $\mathbf{Pb^{2+}}$, the absorbance at 281 nm decreased regularly along with the increase of a new absorption peak at $\lambda_{max} = 371$ nm (Fig. 3a). This change was associated with the appearance of one isosbestic point at 330 nm indicating the complex formation reaction. No positive response of **HQP** was found for other cations in the UV-vis absorption spectra (Fig. 4a). For the calculation of association constant (K) using the nonlinear method,[19] the intensity of the UV-vis absorption (I) of **HQP** at 281 nm was plotted against the concentration of $\mathbf{Pb^{2+}}$ following the non-linear curve fitting

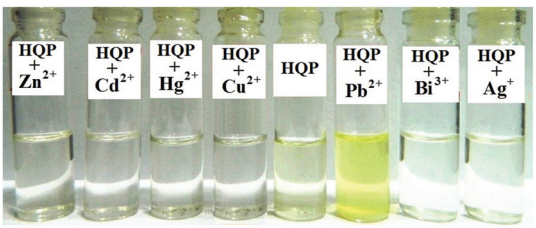

Fig. 2 Visual colour change of **HQP** ($c = 2.085 \times 10^{-4}$ M) with different cations in CH_3OH–H_2O (1 : 1).

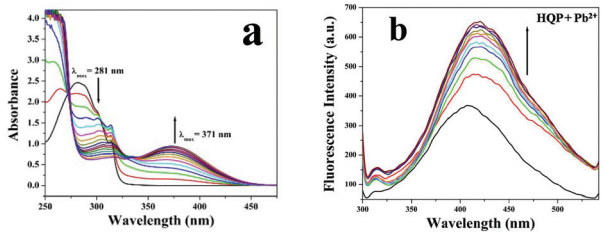

Fig. 3 (a) UV-Vis absorption spectra and (b) fluorescence emission spectra of **HQP** with $\mathbf{Pb^{2+}}$ ($\lambda_{exc} = 281$ nm), in a CH_3OH–H_2O (1 : 1) solvent.

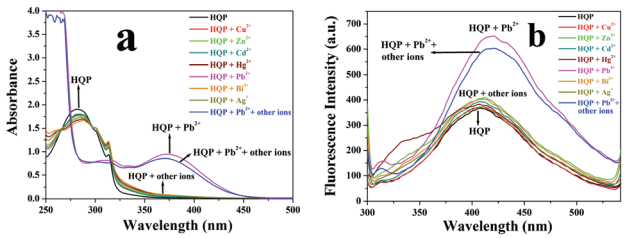

Fig. 4 Competitive (a) UV-Vis and (b) fluorescence spectral experiments of **HQP** with Pb^{2+} and other ions.

equation: $Y = (I_0 + AKX)/(1 + KX)$, where $X = [Pb^{2+}]$, Y = intensity of UV Vis absorption, I_0 = initial intensity of **HQP**. The very high association constant value ($K = 1.23 \times 10^5\ M^{-1}$) of **HQP** with Pb^{2+} (see ESI†) suggested a strong interaction between them.

Complexation study using fluorescence experiments

The complexation study of **HQP** with different cations was also carried out by fluorescence spectroscopic analysis in CH_3OH–H_2O (1 : 1). When a solution of **HQP** (2.085×10^{-4} M) was excited at λ_{max} = 281 nm, an emission spectrum with peak maxima at 407 nm was obtained. Sharp fluorescence enhancement with a slight peak shift from 407 nm to 420 nm was found for **HQP** in the presence of Pb^{2+} (Fig. 3b) only. The fluorescence response of **HQP** with other cations was not significant enough (Fig. 4b). The limit of detection (LOD) calculation[20] using fluorescence experiments pointed out that **HQP** could sense Pb^{2+} up to a very low concentration (1.47×10^{-7} M) (see ESI†).

The competitive experiment using the UV-vis and fluorescence methods was also performed and confirmed no such interference by other metal ions in the colorimetric and fluorescence response of **HQP** to Pb^{2+} (Fig. 4).

pH titration experiment

To investigate the practical applicability, the effect of pH on the UV-vis and fluorescence intensities of **HQP** in the presence and absence of Pb^{2+} were studied at different pH conditions (pH 1.0 to 12.0). Fig. 5 shows that the intensity of free **HQP** increases from acidic to neutral conditions and remained almost the same in basic conditions, which suggested that **HQP** had very good sensitivity in the neutral to basic region and the least sensitivity in acidic conditions. This was probably due to the phosphoester bond cleavage resulting in lower conjugation. But the present scenario changed totally when Pb^{2+} was introduced with **HQP**, where both the UV-vis and fluorescence intensities were very high in acidic conditions (pH 1 to 6) because acidic conditions were favorable for phosphoester hydrolysis of **HQP** for the formation of the $Pb_4(HQ)_6$ complex. The intensity changes of the complex were negligible from pH 7 to 12 as the basic conditions had no effect on complex formation. The pH titration curves also suggested that the UV-vis absorbance intensity of the complex was lower than that of **HQP** but the fluorescence intensity of the complex was higher than that of **HQP**.

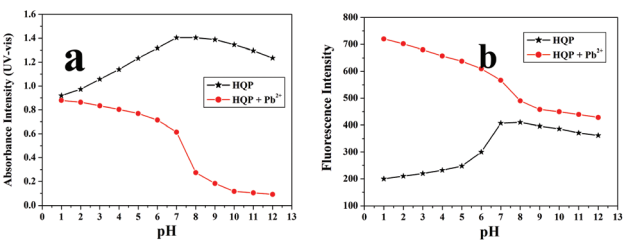

Fig. 5 pH titration curve for (a) the UV-vis absorbance intensity (at 281 nm for free **HQP** and 371 nm for **HQP** + Pb^{2+}) and (b) the fluorescence intensity at 407 nm (λ_{ex} = 281 nm) of **HQP** in the presence and absence of Pb^{2+} at different pH conditions (pH 1.0–12.0).

Probable mechanism for complex formation

The chemodosimeter approach of **HQP** with Pb^{2+} was proposed from the above results as the colourless solution of **HQP** was turned into a visually detectable greenish-yellow colour due to the formation of a ligand–metal charge transfer complex[21] through phosphoester (P–O) bond cleavage and the formation of new Pb–O and Pb–N bonds. This P–O bond breaking process was initiated by the hydrolysis reaction of the phosphoester compound (**HQP**) by the nucleophilic attack of solvent water (Scheme 2). The role of ring N-atoms in the quinoline moiety was very crucial in the bond cleavage reaction as it provided an extra force for the breaking of P–O bonds in **HQP** through complexation with Pb^{2+}. The interaction of the N and O atoms of the quinoline moiety with Pb^{2+} facilitated the charge transfer (CT) process from the heterocyclic quinoline ring to the lead ion. It indeed pronounced the enhancement of electrophilicity to the central P atom to make it easier for the nucleophilic attack of water. This observation was proven when we compared the whole experiment using naphthol phosphate (**NP**) as a dummy molecule. No such metal ion induced phosphor-ester bond cleavage had taken place with no characteristic colour change due to the absence of a ring N atom in the naphthalene moiety. This observation was also helpful for the selective detection of Pb^{2+} by **HQP** in the presence of other heavy metal ions.

Quantum chemical DFT calculation

For the support of experimental work, quantum chemical (DFT) calculations were performed using the Gaussian 09[22]

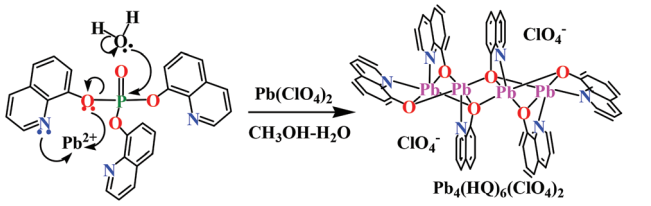

Scheme 2 Complex formation reaction of **HQP** with Pb^{2+}.

program package with the aid of the Gauss-View 5.0[23] visualization program. The structures of the compounds were optimized using Density Functional Theory (DFT) and B3LYP procedures[24] in the restricted forms, following 6-31G and LanL2MB basis sets. DFT calculations and molecular modelling studies determined the energy optimized structures and electronic properties of the phospho-esters. The energy minimised structures of **HQP** and **NP** showed that the three quinoline and naphthalene moieties were located apart from each other, similar to the single crystal X-ray structures of **HQP** and **NP** (Fig. 6). The two-dimensional stable network structure of $\mathbf{Pb_4(HQ)_6}$ displayed that four lead(II) ions were co-ordinated by six hydroxyquinoline(HQ) moieties through Pb–O and Pb–N bonds, where all four lead atoms were penta co-ordinated (Fig. 6).

Molecular Electrostatic Potential (MEP) map diagrams of the compounds highlighted the most negative regions in a deep red colour and positive regions in a blue colour (Fig. 6). The red coloured negative regions were located mainly around the O and N atoms of **HQP**. The appearance of these negative regions around the O and N atoms of **HQP** encouraged $\mathbf{Pb^{2+}}$ to participate in P–O bond breaking reactions. This negative region around the naphthalene ring was absent for **NP**, which made **NP** inert in the reactions with metal ions.

Theoretically calculated highest occupied molecular orbitals (HOMOs) and the lowest unoccupied molecular orbitals (LUMOs) of **HQP** and $\mathbf{Pb_4(HQ)_6}$ were represented in Fig. 7. It was suggested that the HOMOs were located around the quinoline ring including O and N atoms. On the other hand, the LUMOs were present mainly around the electropositive central P atom. HOMO–LUMO structures of $\mathbf{Pb_4(HQ)_6}$ suggested that the electronic transition took place from electronegative O and N atoms of the quinoline moiety to the electropositive $\mathbf{Pb^{2+}}$ ions. The extra electron donating capability of the quinoline N atoms facilitated P–O bond breaking through coordination with $\mathbf{Pb^{2+}}$.

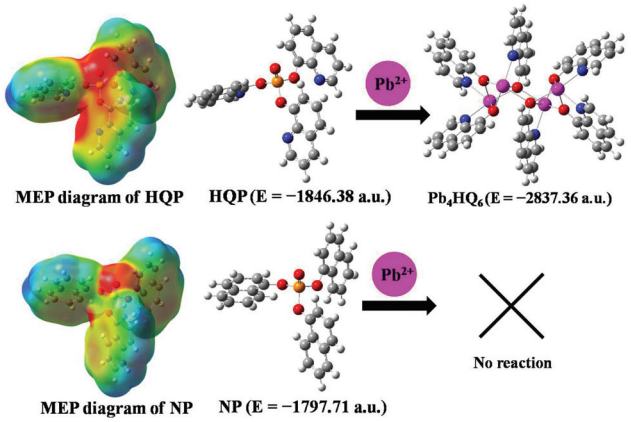

Fig. 6 Optimized structure of **HQP**, **NP** and $\mathbf{Pb_4(HQ)_6}$ and MEP map diagrams of **HQP** and **NP** by DFT/B3LYP/6-31G and LanL2MB method.

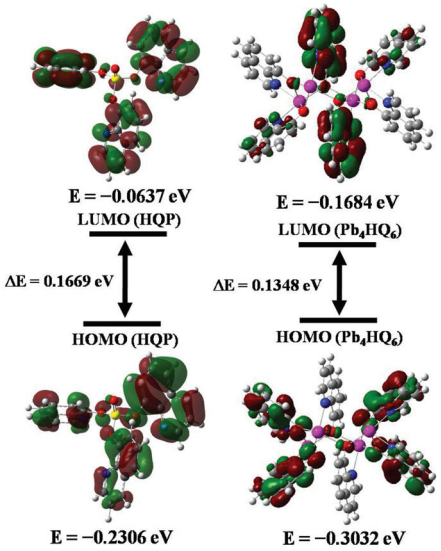

Fig. 7 HOMO and LUMO diagrams of **HQP** and **NP** with their orbital energies.

Conclusions

In conclusion, two phospho-ester compounds (**HQP** and **NP**) based on 8-hydroxyquinoline and 1-naphthol moieties were individually designed and synthesized. The single crystal X-ray crystallographic analysis showed the actual solid state stable structures of the **HQP**, **NP** and $\mathbf{Pb_4(HQ)_6(ClO_4)_2}$ complexes. The three-dimensional network of the $\mathbf{Pb_4(HQ)_6(ClO_4)_2}$ complex proved the hydrolysis of **HQP** followed by phosphoester (P–O) bond cleavage under the influence of $\mathbf{Pb^{2+}}$ ions. The formation of new 'Pb–O' and 'Pb–N' bonds associated with colour change from colourless to yellowish green upon addition of $\mathbf{Pb^{2+}}$ ions was observed. The bathochromic shift of **HQP** (λ_{max} 281 to 371 nm with $\mathbf{Pb^{2+}}$) and isobestic point formation found in the electronic spectra strongly supported the complex formation selectively with $\mathbf{Pb^{2+}}$. All of the above results concluded the chemodosimeter approach of **HQP** selectively towards $\mathbf{Pb^{2+}}$ ions. The complexation with a dummy phospho-ester compound (**NP**) did not show any response towards complexation with metal cations due to the absence of N. The structural aspects of these compounds were investigated by quantum chemical calculations with MEP diagrams for the optimization of stable structures and HOMO–LUMO interactions.

Experimental

All reagents (AR grade) for synthesis were obtained commercially and used without further purification. Solvents were dried following standard procedures. UV-grade CH_3OH was used for the UV-vis and fluorescence titrations. ^1H NMR spectra were recorded on a Bruker AV400 instrument at 400 MHz with TMS as an internal standard. ESI-MS measure-

ments were carried out using a microTOF-Q II 10330 mass spectrometer. IR spectra were measured using a Spectrum 2000 Perkin-Elmer Spectrometer. UV–Vis spectra and Fluorescence spectra were recorded using a UV-1800 Shimadzu Spectrophotometer (1.0 cm quartz cell) and Perkin-Elmer LS 55 Fluorescence spectrometer, respectively. Melting points were determined using Remco hot-coil stage melting point apparatus and are uncorrected.

General procedure for the synthesis of hydroxyquinoline phosphate (HQP) and naphthol phosphate (NP)

8-Hydroxyquinoline (1.42 g, 9.78 mmol) was dissolved in 10 ml dry benzene, followed by the addition of dry Et_3N (1 ml). After cooling the system in an ice bath, $POCl_3$ (0.3 ml, 3.26 mmol) was added dropwise for 10 minutes. Then the ice bath was removed and the solution was refluxed for 10 h. After completion of the reaction, monitored by TLC, the benzene solvent was removed under vacuum. Then $CHCl_3$ was added to the reaction mixture and it was filtered. The filtrate was dried and the crude solid was purified using the column chromatography technique using chloroform ($CHCl_3$) as eluent to get pure **HQP**. For the synthesis of **NP**, 1-naphthol (1.41 g, 9.78 mmol) was used instead of 8-hydroxyquinoline and the reaction was carried out in the same way.

Characteristic experimental data of HQP

Melting point: 196–198 °C; **^{1}H NMR (400 MHz, $CDCl_3$):** δ 8.80 (d, J = 4.4 Hz, 3H), 8.20 (d, J = 8.0 Hz, 3H), 8.15 (d, J = 8.4 Hz, 3H), 7.68 (d, J = 8.4 Hz, 3H), 7.54 (t, J = 8.0 Hz, 3H), 7.40 (dd, J = 8.0 Hz, 3H); **^{13}C NMR of R1 (125 MHz, $CDCl_3$):** δ 150.1, 147.0, 140.7, 135.6, 129.5, 126.3, 124.8, 121.6, 120.0; **TOF-MS ES$^+$ (m/z, %):** 480.87 (M + 1, 30), 479.86 (M^+, 100), 334.90 (10); **FT-IR (KBr, cm^{-1}):** 3016 (Ar. C–H str.), 2676, 1600 (Ar. C═N str.), 1488 (Ar. C═C str.), 1301 (Ar. C–O str.), 1251 (P═O str.), 1082, 951 (P–O str.), 841 (Ar. C–H bending).

Characteristic experimental data of NP

Melting point: 148–150 °C; **^{1}H NMR (400 MHz, $CDCl_3$):** δ 7.96 (d, J = 8.5 Hz, 3H), 7.84 (d, J = 8.5 Hz, 3H), 7.71 (d, J = 8.5 Hz, 3H), 7.61 (d, J = 7.5 Hz, 3H), 7.48 (t, J = 8.5 Hz, 3H), 7.41–7.37 (m, 6H); **^{13}C NMR (100 MHz, $CDCl_3$):** δ 146.5, 134.7, 127.7, 126.7, 126.5, 126.2, 125.6, 125.4, 121.4, 115.3; **TOF-MS ES$^+$ (m/z, %):** 499.90 (M + 23, 30), 498.88 (M-1 + 23, 90), 476.92 (M^+, 100); **FT-IR (KBr, cm^{-1}):** 3058 (Ar. C–H str.), 1598 (Ar. C═C str.), 1389, 1299 (Ar. C–O str.), 1222, 1156 (P═O str.), 1077, 1042, 951 (P–O str.), 845 (Ar. C–H bending).

X-ray crystallography

The data of the **HQP**, **NP** and $Pb_4(HQ)_6(ClO_4)_2$ compounds were collected on a Bruker AXS SMART APEX II diffractometer equipped with an area detector system, using Mo Kα radiation with graphite monochromatization (λ = 0.71073 Å) at T = 293 (2) K. The structures were solved by direct methods using SHELXS-97 (Sheldrick, 1990) and refined by the full-matrix least-squares method; using SHELXL-2013 (Sheldrick, 2013). Crystallographic data (excluding structure factors) for the structures reported in this paper have been deposited with the Cambridge Crystallographic Data Centre with supplementary publication no. CCDC 1413010, 1413011 and 1413012. The crystallographic data are summarized in Table S1 (ESI†).

Acknowledgements

DS, CK and AK are sincerely thankful to the Indian School of Mines for the Junior Research Fellowship. SD acknowledges Erusmus Mundus Action 2 AREAS+ for providing Postdoctoral fellowship.

Notes and references

1 F. H. Westheimer, *Science*, 1987, **235**, 1173.
2 (*a*) T. C. Bruice and S. J. Benkovic, *Bio-Organic Mechanisms*, ed. W. A. Benjamin, New York, USA, 1966; (*b*) P. Gillespie, F. Ramirez, I. Ugi and D. Marquarding, *Angew. Chem., Int. Ed. Engl.*, 1973, **12**, 91.
3 (*a*) J. R. Cox Jr. and O. B. Ramsday, *Chem. Rev.*, 1964, **64**, 317; (*b*) C. R. Hall and T. D. Inch, *Tetrahedron*, 1980, **36**, 2059.
4 C. C. P. Wagener, A. M. Modro and T. A. Modro, *J. Phys. Org. Chem.*, 1991, **4**, 516.
5 (*a*) F. H. Westheimer, *Acc. Chem. Res.*, 1968, **1**, 70; (*b*) K. Taira, T. Fanni and D. G. Gorenstein, *J. Org. Chem.*, 1984, **49**, 453; (*c*) G. Aksnes and K. Bergesen, *Acta Chem. Scand.*, 1966, **20**, 2508; (*d*) G. R. Thatcher and D. R. Cameron, *J. Chem. Soc., Perkin Trans. 2*, 1996, 767; (*e*) N.-Y. Chang and C. Lim, *J. Am. Chem. Soc.*, 1998, **120**, 2156; (*f*) C. S. Lopez, O. N. Faza, A. R. de Lera and D. M. York, *Chem. – Eur. J.*, 2005, **11**, 2081.
6 N. Ashkenazi, S. S. Zade, Y. Segall, Y. Kartona and M. Bendikov, *Chem. Commun.*, 2005, 5879.
7 F. Covitz and F. H. Westheimer, *J. Am. Chem. Soc.*, 1963, **85**, 1773.
8 (*a*) B. S. Souza, T. A. S. Brandao, E. S. Orth, A. C. Roma, R. L. Longo, C. A. Bunton and F. Nome, *J. Org. Chem.*, 2009, **74**, 1042; (*b*) D. Barford, A. K. Das and M. P. Egloff, *Annu. Rev. Biophys. Biomol. Struct.*, 1998, **27**, 133; (*c*) M. D. Jackson and J. M. Denu, *Chem. Rev.*, 2001, **101**, 2313.
9 (*a*) H. Sigel, *Inorg. Chim. Acta*, 1992, **1**, 198; (*b*) P. Hendry and A. M. Sargeson, in *Progress in Inorganic Chemistry: Bioinorganic Chemistry*, ed. S. J. Lippard, Wiley, New York, 1990, vol. 38, p. 201.
10 M.-Y. Chae and A. W. Czarnik, *J. Am. Chem. Soc.*, 1992, **114**, 9704.
11 (*a*) D. T. Quang and J. S. Kim, *Chem. Rev.*, 2010, **110**, 6280; (*b*) M. H. Lee, S. W. Lee, S. H. Kim, C. Kang and J. S. Kim, *Org. Lett.*, 2009, **11**, 2101.
12 (*a*) *National Primary Drinking Water Regulations, Code of Federal Regulations*, 40CFR, 2002, ch. 1, vol. 19, p. 141; (*b*) *Guidelines for Drinking-Water Quality*, World Health Organization, Geneva, 2nd edn, 1996, vol. 2, p. 940.

13 (*a*) Centers for Disease Control (U.S.), *Preventing lead poisoning in young children: a statement*, The Centers, Atlanta, GA, 4th revision edn, 1991; (*b*) J. S. Casas and J. Sordo, in *Lead: Chemistry, Analytical Aspects, Environmental Impact and Health Effects*, Elsevier Science, Amsterdam, 1st edn, 2006; (*c*) R. R. Bustos and S. J. Goldstein, *Atten. Disord.*, 2008, **11**, 425; (*d*) L. M. Schell, M. Denham, A. D. Stark, P. J. Parsons and E. E. Schulte, *Am. J. Hum. Biol.*, 2009, **21**, 180; (*e*) W. Jedrychowski, F. Perera, J. Jankowski, V. Rauh, E. Flak, K. L. Caldwell, R. L. Jones, A. Pac and I. Lisowska-Miszczyk, *Int. J. Hyg. Environ. Health*, 2008, **211**, 345; (*f*) C. Sobin, N. Parisi, T. Schaub, M. Gutierrez and A. X. Ortega, *Arch. Environ. Contam. Toxicol.*, 2011, **61**, 521.

14 (*a*) J. Fan, P. Zhan, M. Hu, W. Sun, J. Tang, J. Wang, S. Sun, F. Song and X. Peng, *Org. Lett.*, 2013, **15**, 492; (*b*) X. Lu, Z. Guo, M. Feng and W. Zhu, *ACS Appl. Mater. Interfaces*, 2012, **4**, 3657; (*c*) Y.-K. Yang, K.-J. Yook and J. Tae, *J. Am. Chem. Soc.*, 2005, **127**, 16760; (*d*) B. Zhu, C. Gao, Y. Zhao, C. Liu, Y. Li, Q. Wei, Z. Ma, B. Du and X. Zhang, *Chem. Commun.*, 2011, **47**, 8656; (*e*) Y. Han, C. Yang, K. Wu, Y. Chen, B. Zhou and M. Xia, *RSC Adv.*, 2015, **5**, 16723; (*f*) W. Luo, H. Jiang, K. Zhang, W. Liu, X. Tang, W. Dou, Z. Ju, Z. Li and W. Liu, *J. Mater. Chem. B*, 2015, **3**, 3459; (*g*) M. Kaur, P. Kaur, V. Dhuna, S. Singh and K. Singh, *Dalton Trans.*, 2014, **43**, 5707; (*h*) S. Pal, J. Hatai, M. Samanta, A. Shaurya and S. Bandyopadhyay, *Org. Biomol. Chem.*, 2014, **12**, 1072.

15 D. G. Khandare, H. Joshi, M. Banerjee, M. S. Majik and A. Chatterjee, *RSC Adv.*, 2014, **4**, 47076.

16 (*a*) S. Deo and H. A. Godwin, *J. Am. Chem. Soc.*, 2000, **122**, 174; (*b*) P. Chen, B. Greenberg, S. Taghvi, C. Romano, D. van der Lelie and C. He, *Angew. Chem., Int. Ed.*, 2005, **44**, 2715; (*c*) H. Wang, Y. Kim, H. Liu, Z. Zhu, S. Bamrungsap and W. Tan, *J. Am. Chem. Soc.*, 2009, **131**, 8221; (*d*) C.-V. Liu, C.-C. Huang and H.-T. Chang, *Anal. Chem.*, 2009, **81**, 2383; (*e*) X. Zhu, Z. Liu, L. Chen, B. Qiu and G. Chen, *Chem. Commun.*, 2009, 6050; (*f*) R. Metivier, I. Leray and B. Valeur, *Chem. Commun.*, 2003, 996; (*g*) J. K. Choi, S. H. Kim, J. Yoon, K.-H. Lee, R. A. Bartsch and J. S. Kim, *J. Org. Chem.*, 2006, **71**, 8011; (*h*) S. K. Saha, K. R. Ghosh, W. Hao, Z. Y. Wang, J. Ma, Y. Chiniforooshan and W. J. Bock, *J. Mater. Chem. A*, 2014, **2**, 5024.

17 K. Ghosh, T. Sarkar, A. Majumdar, S. K. Mandal and A. R. Khuda-Bukhsh, *Anal. Methods*, 2014, **6**, 2648.

18 L. N. Neupane, J.-Y. Park, J. H. Park and K.-H. Lee, *Org. Lett.*, 2013, **15**, 254.

19 K. Ghosh and T. Sen, *J. Phys. Chem. B*, 2011, **115**, 8597.

20 (*a*) M. Shortreed, R. Kopelman, M. Kuhn and B. Hoyland, *Anal. Chem.*, 1996, **68**, 1414; (*b*) Y. Yang, T. Cheng, W. Zhu, Y. Xu and X. Qian, *Org. Lett.*, 2011, **13**, 264; (*c*) W. Lin, L. Yuan, Z. Cao, Y. Feng and L. Long, *Chem. – Eur. J.*, 2009, **15**, 5096.

21 A. B. P. Lever, *J. Chem. Educ.*, 1974, **51**, 612.

22 M. J. Frisch, *et al.*, *GAUSSIAN 09, Rev. D.01*, Gaussian, Inc., Wallingford, CT, 2009.

23 R. D. Dennington II, T. A. Keith and J. M. Millam, *GaussView 5.0*, Gaussian, Inc., Wallingford, CT, 2009.

24 (*a*) A. D. Becke, *J. Chem. Phys.*, 1993, **98**, 5648; (*b*) C. Lee, W. Yang and R. G. Parr, *Phys. Rev. B: Condens. Matter*, 1988, **37**, 785; (*c*) A. D. Becke, *Phys. Rev. A*, 1988, **38**, 3098.

